Path-Integral Molecular Dynamics Calculations of Electron Plasma

Ki-dong Oh
Department of Physics, University of Arizona, Tucson, Arizona 85721

P. A. Deymier
Department of Materials Science and Engineering, University of Arizona, Tucson, Arizona 85721
(Received 16 March 1998)

We introduce a first-principles molecular dynamics method based on the discretized path integral representation of quantum particles. Fermi statistics is automatically generated by an effective exchange potential. This path-integral molecular dynamics method is able to simulate exchange in electron plasmas at the border of the degenerate regime with a satisfactory level of accuracy. [S0031-9007(98)07262-7]

PACS numbers: 31.15.Qg, 71.10.Ca

Current *ab initio* molecular dynamics (MD) methods relying on the density functional theory (DFT) within the local density approximation (LDA) [1,2] have enjoyed a great popularity and have been employed to investigate a very large number of problems [3]. In the LDA, the exchange-correlation energy of a nonuniform electron gas is calculated from the exchange-correlation energy of the uniform gas. The calculation of the equation of states of a Fermi one-component plasma (OCP) such as the interacting electron gas is therefore a problem of fundamental and practical importance. The zero-temperature perturbative expansion of the energy of a uniform electron plasma in the high density limit (when r_s, the radius of a sphere which encloses on the average one particle, is much smaller than the Bohr radius, a_0) was calculated quite some time ago [4]. Accurate Monte Carlo variational calculations have extended the $T = 0$ K equation of states of the degenerate Fermi OCP to a wide range of lower densities, $r_s/a_0 \in [1500]$ [5]. The exchange-correlation free energy has been subsequently calculated to encompass the full range of thermal degeneracy [6–8]. In contrast to DFT-MD, quantum molecular dynamics simulations using the discretized path integral [9] have been limited mostly to the simulation of systems containing a small number of quantum degrees of freedom such as in the solvation of a single quantum particle in a classical fluid [10] or to problems where quantum exchange is not dominant [11]. Progresses in the simulation of fermionic systems by path-integral Monte Carlo [12–15] have opened the way toward the implementation of a path-integral-based finite-temperature *ab initio* molecular dynamics method (PIMD). This Letter describes such a molecular dynamics method applicable to the simulation of many fermion systems at finite temperatures. It is applied to the description of the electron plasma at the border of the degenerate regime where the ratio of the temperature to the Fermi temperature $T_F \approx 0.1$. The method is based on (a) the discretized path integral representation of quantum particles as closed "polymeric" chains of classical particles (beads) coupled through harmonic springs [9], (b) the treatment of quantum exchange as crosslinking of the chains [16], (c) the nonlocality of crosslinking (exchange) along the chains (in imaginary time) [12], (d) the restricted path integral [13,17] to resolve the problem of negative weights to the partition function resulting from the crosslinking of even numbers of quantum particles.

The partition function of a system of N quantum particles expressed in a position representation takes the form [18]

$$Z = \int dR_1\, \rho(R_1, R_1; \beta) = \int \prod_{n=1}^{P} dR_n \prod_{n=1}^{P}{}^{*} \rho(R_n, R_{n+1}; \varepsilon)\,, \qquad (1)$$

where ρ is the density matrix, $R = \{\mathbf{r}^{(1)}, \ldots, \mathbf{r}^{(N)}\}$ stands for the position of the particles, and $\beta = 1/\mathrm{kT}$. In Eq. (1), we have used the convolution property of the density matrix and introduced $(P - 1)$ intermediate states. The $(*)$ in the product indicates the cyclic condition $R_{P+1} = R_1$ and $\varepsilon = \beta/P$. Since the wave function of fermions is antisymmetric, the density matrix can be positive or negative and convergence is slow. However, the diagonal density matrix can be evaluated by restricting paths to remain in the region of phase space where their sign is positive [13]. With this restriction, Eq. (1) is exact, but since one does not know the exact density matrix, it is necessary to replace it by some reasonable approximation. The nodes (loci of points where the density matrix is zero) of the approximate density matrix should be as close as possible to those of the exact density matrix if one hopes to calculate accurate properties. If P is sufficiently large, we can use Trotter's approximation to separate the kinetic and the potential contributions to the density matrix [19]. The kinetic density matrix may then be approximated by a local form of the noninteracting density matrix.

$$\rho_{\mathrm{NI}}(R_n, R_{n+1}; \varepsilon) = \left[\frac{m}{2\pi\varepsilon\hbar^2}\right]^{3N/2} \det[A_{n,n+1}]\,. \qquad (2)$$

 0031-9007/98/81(15)/3104(4)$15.00

$[A_{n,n+1}]$ represents a $N \times N$ matrix which elements are expressed as

$$A^{ij}_{n,n+1} = \exp\left[-\beta \frac{m}{2\beta\varepsilon\hbar^2} (r_n^{(i)} - r_{n+1}^{(j)})^2 \right]$$

with the indices i and j running over the particles. In the limit of high temperature, the nodes of the noninteracting density matrix approximate reasonably well those of the exact density matrix [13], although it does not describe electron correlation. The determinant of the kinetic matrix in the absence of quantum exchange is factored out of Eq. (2)

$$\det[A_{n,n+1}] = \prod_{i=1}^{N} A^{ii}_{n,n+1} \det[E_{n,n+1}], \qquad (3)$$

where all the exchange effects (including the sign of the density matrix) are included in $[E]$ which elements are defined as $E^{ij}_{n,n+1} = A^{ij}_{n,n+1}/A^{ii}_{n,n+1}$. In the limit of $\varepsilon \to 0$, the matrix $[E]$ reduces to the identity matrix and the system collapses into a bosonic state. To prevent this undesirable behavior, we recast Eq. (3) in a nonlocal form [12]:

$$\det[A_{n,n+1}] = \prod_{i=1}^{N} A^{ii}_{n,n+1} \prod_{m=1}^{P} (\det[E_{n,m}])^{1/P}. \qquad (4)$$

With the restricted path integral, the integrand of the partition function is positive and Z can now be rewritten in a classical form usable with a molecular dynamics (MD) scheme

$$Z = \int \prod_{n=1}^{P} dR_n \exp[-\beta V_{\text{eff}}(R_1, \ldots, R_P)], \qquad (5)$$

where the effective potential includes quantum exchange. In the case of a nonpolarized fermion system with N_{el} electrons, a microcanonical ensemble sampling of the quantum states of the system can now be performed by solving for the trajectories generated by the classical Hamiltonian:

$$H = \sum_{k=1}^{N_{\text{el}}} \sum_{i=1}^{P} \frac{1}{2} m^* (\dot{r}_i^{(k)})^2 + \sum_{i=1}^{P} \sum_{k>1}^{N_{\text{el}}} \sum_{l=1}^{N_{\text{el}}-1} \frac{(-e)(-e/P)}{4\pi\varepsilon_0 |r_i^{(k)} - r_i^{(l)}|} + \sum_{k=1}^{N_{\text{el}}} \sum_{i=1}^{P} {}^{*} \frac{m_e P}{2\hbar^2\beta^2} (r_i^{(k)} - r_{i+1}^{(k)})^2 - \frac{1}{\beta} \sum_{s=\uparrow}^{\downarrow} \frac{\sum_{i=1}^{P} \sum_{j=1}^{P} \ln \det[E_{ij}]_s \theta^+_{ijs}}{\sum_{i=1}^{P} \sum_{j=1}^{P} \theta^+_{ijs}}. \qquad (6)$$

Here, m^* is some arbitrary mass (we chose $m^* = 1$ a.u.) used to define an artificial kinetic energy for the quantum states in order to explore the effective potential surface, V_{eff}, constituted of the last three terms in Eq. (6). The fourth term is an effective exchange potential for the electrons with spin-up ($s = \uparrow$) and spin-down ($s = \downarrow$). The function θ^+_{ij} ensures the path restriction by taking on the values 1 and 0 for paths with positive and negative $\det[E]$, respectively. In Eq. (6), the second term accounts for the electron/electron Coulomb interactions. The forces derived from the exchange potential are calculated as means over the paths with positive determinant. Therefore, an effective force calculation requires a good sample of such paths. Since the exchange potential offers a barrier to paths with negative determinants, it biases the sampling of phase space toward configurations with positive determinants. Although configurations with negative determinants exist and evolve, they do not contribute to the exchange forces.

We have tested the PIMD on an unpolarized electron plasma composed of $N_{\text{el}} = 30$ electrons ($N_\uparrow = 15$ and $N_\downarrow = 15$). The simulation cell is a fixed cubic box with edge length $L = 13.3$ Å, which corresponds to an electronic density with $r_s/a_0 = 5$. This electron density is near that of some metallic systems. Three temperatures are considered, 1300, 1800, and 2300 K, giving ratios T/T_{F} in the interval $[0.05, 0.1]$. Periodic boundary conditions are used. Under these conditions the matrix $[E_{n,m}]$ for each spin s should be a $(27N_s \times 27N_s)$ matrix since there are 26 periodic image cells and one simulation cell. In order to make the calculation more tractable, at every time step, we approximate the matrix $[E_{n,m}]$ by a block diagonal matrix containing two blocks. The first block $[F_{n,m}]$ is a $N_s \times N_s$ matrix which elements minimize the quantity $|(\mathbf{r}_n^{(i)} - \mathbf{r}_m^{(j)})^2 + (\mathbf{r}_n^{(j)} - \mathbf{r}_m^{(i)})^2 - (\mathbf{r}_n^{(i)} - \mathbf{r}_m^{(i)})^2 - (\mathbf{r}_n^{(j)} - \mathbf{r}_m^{(j)})^2|$ among the possible combinations of exchange between a particle i in the simulation cell and a particle j in any other cell. This procedure identifies the leading pair exchange terms in $\det[E_{n,m}]$ involving at least one particle in the simulation cell. The second block which determinant will be denoted C contains the contribution of exchange between electrons in the image cells and a minor contribution from exchange processes between electrons in the simulation cells and all other cells. With this approximation, $\det[E_{n,m}] \approx C \det[F_{n,m}]$. When calculating the leading contributions to the exchange force on the electrons inside the simulation cell, as the derivative of the exchange potential of Eq. (6), the quantity C drops out and does not need to be evaluated. This approximation should be valid at high temperature when the electrons are fairly well localized and for systems in which the electrons have a strong repulsive interaction that prevents the close approach of more than a very few electrons at a time.

We solve the equation of motion with a leap frog scheme with a time step of 1.35×10^{-16} sec with simulations lasting at least 16 000 time steps. The time step is small enough to resolve the high frequency oscillations of the harmonic springs. In the case of systems with large P, the strong harmonic forces in Eq. (6) may lead to nonergodic behaviors [20]. This problem can be alleviated by

rescaling temperature with a chain of Nosé-Hoover thermostats [11,21]. This rescaling would ensure convergence to the right canonical distribution. We have elected to rescale the temperature of each chain of P beads independently of each other via a momentum rescaling thermostat [22]. With this procedure we do not obtain a true canonical distribution, but most thermal averages will be accurate to orders N^{-1} [23]. We have also verified that with this approach over the length of our simulations the chains would sample a large region of configuration space and therefore resolve not only the fast but also the slow dynamical scale.

The calculation of the Coulomb energy is handled by the usual Ewald method of summation. The Coulomb potential energy of the electron plasma is made convergent by the introduction of a positive charged background of density $-30e/\Omega$ where Ω is the cell volume. We calculate the kinetic energy with the usual energy estimator derived from $\partial \ln Z/\partial\beta$ [10].

Every simulation reported starts with a different initial configuration obtained from randomly generated bead position in every electron chain. The initial bead-bead distance is determined by the temperature. We have checked that simulations at the same temperature starting from different initial configurations lead to the same equilibration state. The rate at which equilibrium is reached, however, may vary with the initial configuration.

We have investigated the convergence of the algorithm with respect to the number of beads at the lowest temperature of 1300 K. The electron plasma exhibits convergence for $P \geq 400$. We have chosen $P = 450$ to ensure convergence at all temperatures greater than 1300 K. In Figs. 1(a) and 1(b) we report the results of our calculations for the kinetic and potential energies of the fermion plasma as a function of temperature as well as the kinetic energy of a similar system but obeying Maxwell-Boltzmann statistics [simulated by switching off the exchange potential in Eq. (6)]. In addition to our results, we present the 0 K kinetic energy of the correlated fermion plasma of Ref. [5] as well as the free electron kinetic energy and the Coulomb contribution of the Hartree-Fock energy. The effectiveness of our exchange potential at all temperatures studied is clearly seen in the magnitude of the fermion kinetic energies. The calculated fermion kinetic energy exceeds the Maxwell-Boltzmann energy by more than 1 eV. This increase in kinetic energy is indicative of a significant localization when the quantum particles obey Fermi statistics. The calculated kinetic energy for the high density fermion system does not show a significant temperature dependency as would be expected for plasmas at the border of the degenerate regime [7]. In contrast, the Maxwell-Boltzmann particles do show a significant temperature dependency for their kinetic energy. The fermion kinetic energies calculated with the PIMD are in very good agreement with Ceperley's results (Ref. [5]) at 0 K although somewhat smaller by approximately 0.05 eV/electron. Our model appears to overestimate

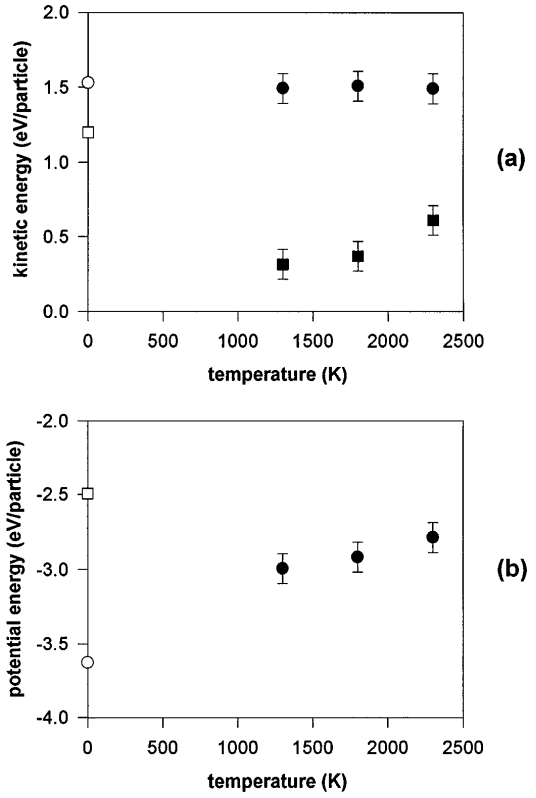

FIG. 1. Kinetic energy (a) and potential energy (b) versus temperature. The open circles are the results of Ref. [5] for a correlated electron plasma. The open squares are the free electron kinetic energy and Hartree-Fock Coulomb contribution to the energy. The closed circles refer to the fermion plasma studied in this paper. The closed squares indicate the kinetic energy of a system composed of Maxwell-Boltzmann particles.

the potential energy of the plasma. However, the PIMD energies are lower than the Coulomb contribution to the Hartree-Fock energy. The deviation from the correlated potential energy may be imputed to the fact that the PIMD presented here does not include explicitly correlation. Incorporation of correlation via a correlated density matrix [24], including some appropriate repulsive long-range pseudopotential [5], should keep the electrons farther apart thus reducing their potential energy. The agreement between the kinetic energy of the PIMD fermion system and that of the correlated electron plasma [5] suggests that the nonlocal form of the effective potential in Eq. (6) may also include some correlation between the electrons in an implicit form [12].

The computing time for the calculation of the exchange potential scales as $P^2 N_{\uparrow,\downarrow}^3$. This scaling at present limits the applicability of the method to systems with a reasonably small number of fermions. However, one may exploit the natural parallelizability of the exchange effective potential over the number of beads to reduce the cost to a linear scaling with respect to P [25]. Access to supercomputers can make possible the simulation of larger systems at lower temperatures. For larger fermion systems, one

may be able to optimize the calculation by using the short spatial extent of exchange [26] and dividing the simulation cell into smaller and more tractable subcells. Extension of the restricted-PIMD method to include classical ionic degrees of freedom is straightforward provided the electrons interact with the ions via local pseudopotentials.

[1] R. Car and M. Parrinello, Phys. Rev. Lett. **55**, 2471 (1985).
[2] A. Selloni, P. Carnevali, R. Car, and M. Parrinello, Phys. Rev. Lett. **59**, 823 (1987).
[3] M. Parrinello, Solid State Commun. **102**, 107 (1997).
[4] M. Gell-Mann and K. Bruekner, Phys. Rev. **106**, 364 (1957).
[5] D. M. Ceperley, Phys. Rev. B **18**, 3126 (1978); D. M. Ceperley and B. J. Alder, Phys. Rev. Lett. **45**, 566 (1980).
[6] F. Perrot and M. W. C. Dharma-wardana, Phys. Rev. A **30**, 2619 (1984).
[7] R. G. Dandrea, N. W. Ashcroft, and A. E. Carlsson, Phys. Rev. B **34**, 2097 (1986).
[8] S. Tanaka, S. Mitake, and S. Ichimaru, Phys. Rev. A **32**, 1896 (1985).
[9] R. P. Feynman and A. R. Hibbs, *Quantum Mechanics and Path Integrals* (McGraw-Hill, New York, 1965).
[10] M. Parrinello and A. Rahman, J. Chem. Phys. **80**, 860 (1984).
[11] D. Marx and M. Parrinello, Z. Phys. B **95**, 143 (1994).
[12] R. W. Hall, J. Chem. Phys. **89**, 4212 (1988); **93**, 5628 (1989); **91**, 1926 (1989).
[13] D. M. Ceperley, Phys. Rev. Lett. **69**, 331 (1992).
[14] D. M. Ceperley, Rev. Mod. Phys. **67**, 279 (1995).
[15] S. Zhang, J. Carlson, and J. E. Gubernatis, Phys. Rev. B **55**, 7464 (1997).
[16] D. Chandler and P. G. Wolynes, J. Chem. Phys. **74**, 4078 (1981).
[17] D. M. Ceperley, J. Stat. Phys. **63**, 1237 (1991).
[18] R. P. Feynman, *Statistical Mechanics* (Benjamin, New York, 1972).
[19] H. Kleinert, *Path Integral in Quantum Mechanics, Statistics, and Polymer Physics* (World Scientific, Singapore, 1990).
[20] R. W. Hall and B. J. Berne, J. Chem. Phys. **81**, 3641 (1984).
[21] G. J. Martyna, M. L. Klein, and M. Tuckerman, J. Chem. Phys. **97**, 2635 (1992).
[22] L. V. Woodcock, Chem. Phys. Lett. **10**, 257 (1971).
[23] M. J. Gillan, in *Computer Modelling of Fluids, Polymers and Solids*, edited by C. R. A. Catlow *et al.* (Kluwer Academic, Dordrecht, 1990), p. 155.
[24] G. Senger, M. L. Ristig, C. E. Campbell, and J. W. Clark, Ann. Phys. (N.Y.) **218**, 160 (1992).
[25] Ki-dong Oh and P. A. Deymier (to be published).
[26] X. P. Li, R. W. Numes, and D. Vanderbilt, Phys. Rev. B **47**, 10 891 (1993).